Journal Pre-proof

$NaCa_4V_5O_{17}$: A low-firing microwave dielectric ceramic with low permittivity and chemical compatibility with silver for LTCC applications

Changzhi Yin, Chunchun Li, Guangjie Yang, Liang Fang, Yonghai Yuan, Longlong Shu, Jibran Khaliq

PII: S0955-2219(19)30639-9

DOI: https://doi.org/10.1016/j.jeurceramsoc.2019.09.029

Reference: JECS 12739

To appear in: *Journal of the European Ceramic Society*

Received Date: 5 July 2019

Revised Date: 12 September 2019

Accepted Date: 15 September 2019

Please cite this article as: Yin C, Li C, Yang G, Fang L, Yuan Y, Shu L, Khaliq J, $NaCa_4V_5O_{17}$: A low-firing microwave dielectric ceramic with low permittivity and chemical compatibility with silver for LTCC applications, *Journal of the European Ceramic Society* (2019), doi: https://doi.org/10.1016/j.jeurceramsoc.2019.09.029

$NaCa_4V_5O_{17}$: A low-firing microwave dielectric ceramic with low permittivity and chemical compatibility with silver for LTCC applications

Changzhi Yin[2], Chunchun Li[1, 2, 3*], Guangjie Yang[1], Liang Fang[2], Yonghai Yuan[3], Longlong Shu[4] and Jibran Khaliq[5**]

[1]*College of Information Science and Engineering, Guilin University of Technology, Guilin, 541004, China*

[2]*Guangxi universities key laboratory of non-ferrous metal oxide electronic functional materials and devices, College of Material Science and Engineering, Guilin University of Technology, Guilin, 541004, China*

[3]*Guangxi Key Laboratory of Hidden Metallic Ore Deposits Exploration，Guilin University of Technology，Guilin, 541004，China;*

[4]*School of Materials Science and Engineering, Nanchang University, Nanchang 330031, People's Republic of China*

[5]*Department of Mechanical and Construction Engineering, Faculty of Engineering and Environment, Northumbria University at Newcastle, NE1 8ST, UK*

Abstract:

Phase formation, crystal structure and dielectric properties of $NaCa_4V_5O_{17}$ ceramics fabricated via a solid state reaction route at relatively low temperatures (780-860 °C) were investigated. $NaCa_4V_5O_{17}$ crystallizes in a triclinic structure. Dielectric properties were measured based on the Hakki-Coleman post resonator method at microwave frequency. Specially, a specimen sintered at 840 °C demonstrated balanced dielectric properties with a permittivity ε_r = 9.72, a quality factor $Q \times f$ = 51,000 GHz, and a temperature coefficient of resonance frequency τ_f = -84 ppm/°C. $NaCa_4V_5O_{17}$ ceramics showed excellent chemical compatibility with Ag metal electrodes. Besides, the thermal stability of resonance frequency was effectively

Authors to whom correspondence should be addressed: *lichunchun2003@126.com
**Jibran.khaliq@northumbria.ac.uk

adjusted through formation of composite ceramics between $NaCa_4V_5O_{17}$ and TiO_2 and a near-zero τ_f ~ 1.3 ppm/°C accompanied with ε_r = 14.9 and $Q \times f$ = 19,600 GHz was achieved when 50% mol TiO_2 was added. All the merits render $NaCa_4V_5O_{17}$ a potential candidate for multilayer electronic devices.

Keywords: Ceramics; Dielectric properties; LTCC; $NaCa_4V_5O_{17}$

1. Introduction

Nowadays, electronic devices have witnessed a constant decrease in the geometrical dimensions of the devices, or in other words, they are being miniaturized. For wireless communication systems, such as a mobile phone, a substantial reduction in sizes (devices or electronic components) have been experienced. The ever-accelerated requirements for miniaturization exert an increasing demand for material exploitation and device design. One direction for device miniaturization is the utilization of high-permittivity (ε_r) materials because the size of the dielectric resonator is inversely proportional to the permittivity [1, 2]. Nevertheless, the dielectric loss, necessary for noise reduction and controlling the cross-talks, inversely correlates to the dielectric permittivity, which makes the high-ε_r materials practically unfavorable in the high-frequency fields. Moreover, high-ε_r materials generally possess a relatively high temperature coefficient of permittivity that is disadvantageous for the thermal stability of devices.

In addition to exploring high-ε_r materials for miniaturization and integration, current research interest has been directed to low-temperature co-fired ceramics (LTCC) technology to integrate a versatile mix of passive components such as

antennas, filter, resonators, and capacitors within a monolithic bulk module [3-6]. Thus, to achieve co-firing with inner metal electrodes (e.g. Ag), low sintering temperatures (< 961 ^{o}C, which is the melting point of Ag) should be satisfied along with chemical compatibility between ceramic matrix and electrodes [7-10].

Generally, the addition of low-melting-point glasses and/or sintering aids proved to be a valid method to develop LTCC systems [11]. However, lowering the sintering temperatures is usually coupled with the deterioration in dielectric properties, especially the quality factor. Within the past two decades, ceramics with intrinsically low densification temperatures have been widely researched, enriching the material systems for LTCC technology. Up till now, a great deal of low-firing ceramics has been reported [12-14]. Those materials with low-melting-point constituents, such as B_2O_3 (450 ^{o}C), V_2O_5 (690 ^{o}C), TeO_2 (733 ^{o}C), MoO_3 (795 ^{o}C), Bi_2O_3 (817 ^{o}C), tend to have low sintering temperatures [5, 15-19]. That is because of the mass transfer due to a liquid phase transition. This proves that for state of the art microwave dielectric materials having intrinsically low sintering temperatures and excellent dielectric performances, it is necessary to focus on the materials consisting of low-melting-point constituents.

Recently, an alkaline earth metal vanadate with an alkali ($NaCa_4V_5O_{17}$) was synthesized and characterized for its crystal structure, spectrum properties, and thermal behavior [20]. $NaCa_4V_5O_{17}$ has a triclinic structure, with 3D frameworks of corner-shared VO_4 tetrahedra that enclose cavities occupied by Na^+ and Ca^{2+} cations. The single-phase $NaCa_4V_5O_{17}$ could be obtained after firing it at 600 ^{o}C which makes

$NaCa_4V_5O_{17}$ an excellent candidate for microwave dielectric application having low-temperature firing.

In this work, $NaCa_4V_5O_{17}$ ceramics were prepared via the conventional solid-state reaction route. The microstructure, sintering behaviors and their effects on dielectric properties were studied in details together with the chemical compatibility of $NaCa_4V_5O_{17}$ with silver.

2. Experimental

2.1 Sample preparation

$NaCa_4V_5O_{17}$ ceramics were prepared via a conventional solid-state method using stoichiometric starting materials: $CaCO_3$, Na_2CO_3 (> 99.95%, Guo-Yao Co., Ltd Shanghai, China) and NH_4VO_3 (> 99.9%, Guo-Yao Co., Ltd Shanghai, China). The stoichiometrically weighted powders were mixed through ball-milling in alcohol medium for 6 h. After drying at 120 °C, the resultant powders were calcined at 650 °C for 6 h in air, followed by a second ball milling for 6 h. Green disks were obtained by pressing powder into cylinders (10 mm in diameter and 6 mm in thickness) under a pressure of 80 MPa with polyvinyl alcohol (PVA, 10 vol.%) as s binder. $NaCa_4V_5O_{17}$ pellets were sintered at 780-860 °C for 6 h to optimize the sintering behavior. To suppress evaporation of volatile elements, such as sodium and vanadium, $NaCa_4V_5O_{17}$ ceramics were buried in sacrificial powders of the same composition.

2.2 Characterization

The phase purity and crystal structure were analyzed using X-ray diffraction (Cu*Kα1*, 1.54059 Å, Model X'Pert PRO, PANalytical, Almelo, Holland). The bulk

density was determined by the Archimedes' principle. The surface morphologies of the polished and thermal etched surfaces were observed by scanning electron microscope (FE-SEM, Model S4800, Hitachi, Japan) fitted with an Energy Dispersive Spectroscopy (EDS). The precise composition of the sintered samples was determined using X-Ray Fluorescence Spectrometer (ZSX Primus II, Japan). High-resolution transmission electron microscopy (HRTEM) and the corresponding selected area electron diffraction (SAED) were performed with a JEM-2100 F at an accelerating voltage of 200 kV. The relative permittivity (ε_r) and quality factor ($Q \times f$) were measured via the Hakki-Coleman dielectric resonator method with TE011 mode using a network analyzer (Model N5230A, Agilent Co., Palo Alto, America) and the temperature coefficient of resonant frequency (τ_f) was obtained by recording the temperature shifts of the resonance frequency in the temperature range from 25-85 ^{o}C using a temperature chamber (Delta 9039, Delta Design, San Diego, CA) and the values were calculated as follows:

$$\tau_f(ppm/^{o}C) = \frac{f_2 - f_1}{f_1(T_2 - T_1)} \times 10^6 \qquad (1)$$

where, f_1 and f_2 represent resonant frequencies at temperatures T_1 (25 ^{o}C) and T_2 (85 ^{o}C), respectively.

3. Results and discussion

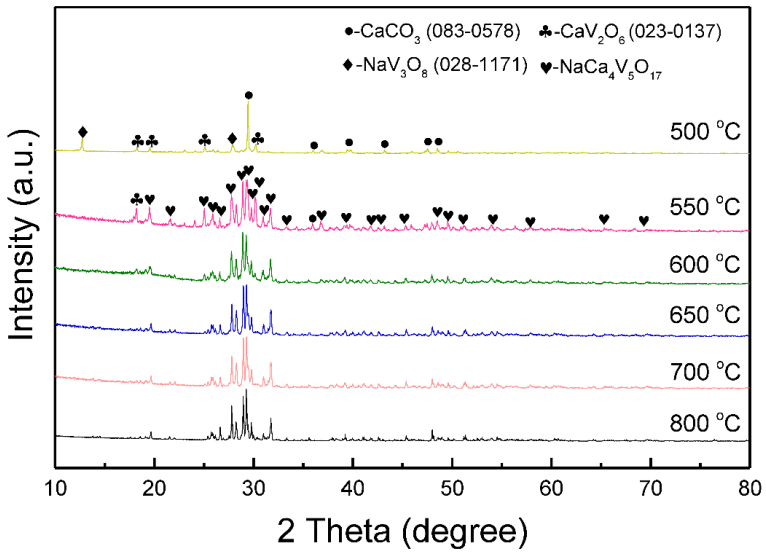

Figure 1 X-ray diffraction profiles recorded on the calcined powders at various temperatures from 500 to 800 °C

Figure 1 shows the XRD profiles of the powders calcined at various temperatures (ranging from 500 to 800 °C). For the sample fired at 500 °C, three main phases indexed as $CaCO_3$ (No. 083-0578), CaV_2O_6 (No. 023-0137), and NaV_3O_8 (No. 028-1171) were detected. This indicates that at low processing temperatures, the primary chemical reactions is decomposition of raw materials to initiate a chemical reaction forming intermediate phases, which was confirmed from thermal analysis and shown in Supplementary Figure 1. With increasing calcination temperature, $NaCa_4V_5O_{17}$ phase began to appear at 550 °C, and eventually became a main phase at 650 °C which kept stable up to 800 °C. Rietveld refinement was performed to determine the crystal structure and to confirm the phase purity based on the powder XRD data collected on the cracked ceramics (sintered at 800 °C).

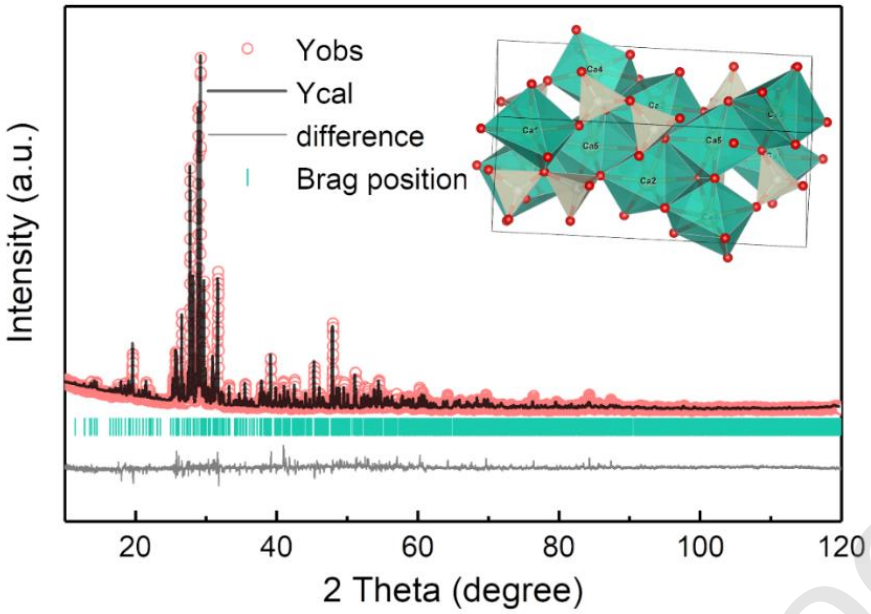

Figure 2 Rietveld refinement on the powder XRD data collected on the cracked ceramics (sintered at 800 ^{o}C) using Fullprof software; the schematic crystal structure of $NaCa_4V_5O_{17}$ is shown in the inset with grey polyhedra for VO_4

A structural model with a space group of *P*-1 was established based on the previous work [20]. The calculated XRD pattern matched well with the observed pattern and shown in Figure 2. The comparison gives a relatively low difference profiles and acceptable reliability factors of the profile R_p = 11.51%, and the weighted profile R_{wp} = 9.39%, which verifies the refinement reliability and phase purity of the sample. The lattice parameters were refined as a = 6.9368 Å, b = 6.9523 Å, c = 15.4928 Å, α = 84.5550^{o}, β = 87.2871^{o}, and γ = 86.8512^{o}. The refined atomic positions are summarized in Supplementary Table 1. A high resolution transmission electron microscopy (HRTEM) image and the corresponding selected area electron diffraction (SAED) pattern acquired along the crystallographic [100] direction (Supplementary Figure 2) further confirmed the triclinic crystal structure. The crystal

structure of $NaCa_4V_5O_{17}$ is shown in the inset of Fig. 2, which features a 3D network of corner-shared VO_4 tetrahedra with Na and Ca occupying the interstitial sites having seven-coordination and/or six-coordination with oxygen.

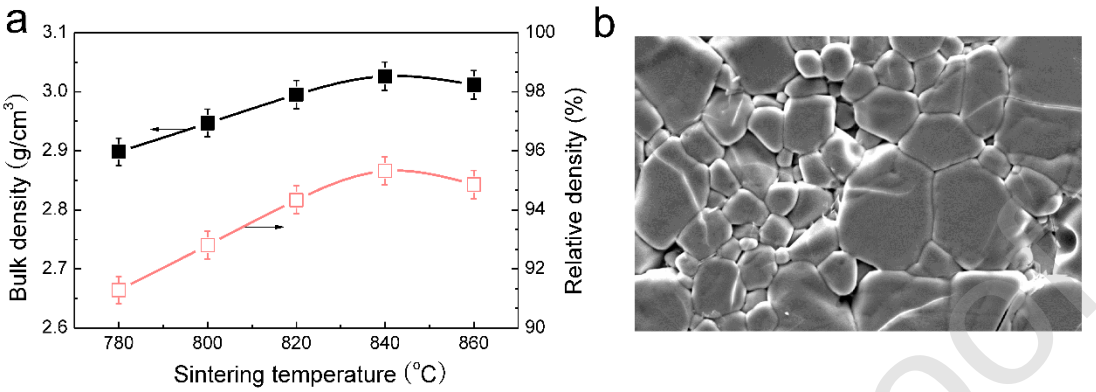

Figure 3 (a) Density of the sintered $NaCa_4V_5O_{17}$ ceramics at various temperatures from 780 to 860 °C with an increment of 20 °C; (b) SEM image of$NaCa_4V_5O_{17}$ ceramic sintered at 840 °C

X-Ray Fluorescence Spectrometer (XRF) was employed to precisely determine the chemical constitution of $NaCa_4V_5O_{17}$ as oxygen loss in oxides frequently occurs and is represented by the KrÖger–Vink notation:

$$O_O \rightleftharpoons 1/2O_2 + V_{\ddot{O}} + 2e' \qquad (1)$$

Inevitably, high-temperature firing would induce evaporation of volatile elements, (such as sodium in the present work) and sodium loss accelerates oxygen deficiency to maintain electrical neutrality. The ionization of oxygen vacancies produces the conducting electrons, which would weakly bond with positively charged defects, resulting in another dielectric polarization. XRF analysis revealed mole ratio for Na:Ca:V = 0.227:1:1.123, which deviated from the stoichiometric ratio (0.25:1:1.125), especially for Na source.

The variation in bulk density and relative density as a function of sintering temperature is presented in Figure 3a. When powder was sintered at 780 ^{o}C, the sample had a relatively low bulk density of 2.9 g/cm^3 (~ 92% of relative density), which increased to a maximum density of 3.03 g/cm^3 (~ 95.3% of relative density) at 840 ^{o}C. Further increase in temperature to 860 ^{o}C, however, led to a decline in bulk density to a value of 3.0 g/cm^3. The increment in density is believed to be due to the grain growth which squeezes out pores as can be seen in Figure 3b which shows the SEM image of sample sintered at 840 ^{o}C. On the other hand, heterogeneous grain growth with increasing sintering temperature is responsible for the decrease in density and the microstructure showing grain growth is given in Supplementary Figure 3 and Supplementary Figure 4.

Figure 4 presents the variation in microwave dielectric properties as a function of sintering temperature. The relative permittivity increased with increasing sintering temperature and reached a saturated value of 9.72 for the sample sintered at 840 ^{o}C. Since, density also exhibited the same trend as permittivity, suggests that the density predominated the relative permittivity of $NaCa_4V_5O_{17}$. It is safe to conclude that the relatively small permittivity of air ($\varepsilon_r \sim 1$) trapped in the pores also contributed to the permittivity values. In order to remove the effect of porosity, Bosman and Having's equation [21] was used which is presented in Eq. 2:

$$\varepsilon_{corr} = \varepsilon_r (1 + 1.5p) \qquad (2)$$

where p is the fractional porosity and ε_{corr} is the corrected value. As expected, the calculated ε_{corr} values were higher (6-10%) than the measured values and presented in

Figure 4a. Additionally, the theoretical permittivity estimated via the Clausius-Mossotti equation was 8.45, which is also different from the measured value (Δ > 10%) [22, 23]. According to Shannon's report, the lower theoretical permittivity (8.45) of $NaCa_4V_5O_{17}$ indicates that there is another contribution to dielectric polarization that relates to ionic or electronic conductivity or stems from the structural distortion with rattling or compressed cations [22].

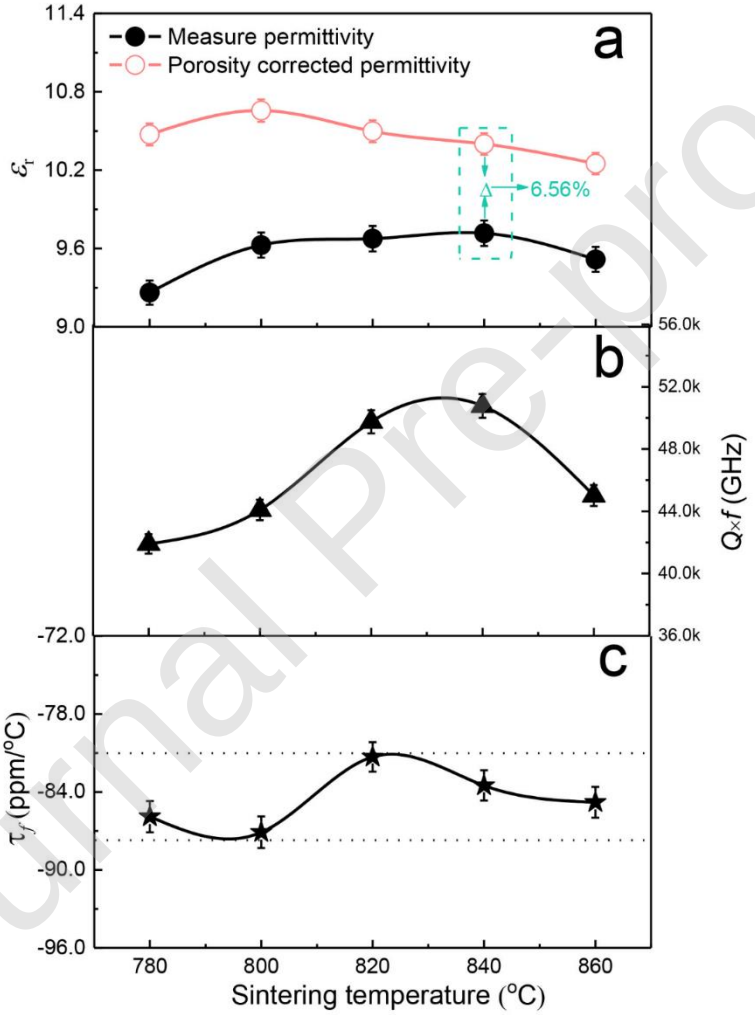

Figure 4 microwave dielectric properties (ε_r, $Q\times f$, and τ_f) of $NaCa_4V_5O_{17}$ ceramics sintered at various temperatures from 780 to 860 °C

Figure 4b shows the quality factor ($Q\times f$) of $NaCa_4V_5O_{17}$ ceramics sintered at various temperatures. For samples sintered at 780 °C, they showed a quality factor

($Q \times f$) of 42,000 GHz, which remarkably improved to 51,000 GHz as the sintering temperature rose to 840 °C. Upon further increasing the temperature to 860 °C, the $Q \times f$ value slightly decreased to 45,000 GHz. A series of factors including intrinsic (such as anharmonic lattice vibration) and extrinsic (related to structural imperfection, e.g. point defects, line defects, and plane defects) have been reported to influence the dielectric losses [24-26]. Considering the similar variation trend between quality factor and density versus the sintering temperature, it is rationally determined that density contributes primarily to the dielectric loss.

As shown in Figure 4c, the temperature coefficient of resonance frequency fluctuated between -87 to -80 ppm/°C for sample sintered between 780 to 860 °C. The weak dependence of τ_f on sintering temperature can originate from the fact that no second phase of structural transformation took place over the same temperature range. **Table 1** summarizes the sintering temperatures and microwave dielectric properties of some previously researched vanadates with ultra-low sintering temperatures. All the listed vanadates have relatively low sintering temperatures (< 960 °C), rendering their possible utilization in LTCC technology. In comparison, this work possesses low relative permittivity, comparable to $Mg_3(VO_4)_2$, which is beneficial for high-speed data propagation. The quality factor of $NaCa_4V_5O_{17}$ is much higher than those of $BiVO_4$ and $LiMVO_6$ (M = Mo and W), which guarantees its high frequency selectivity. However, the low-firing vanadates usually exhibit non-zero τ_f values (either positive or negative), which needs further compensation mechanisms to tune.

Table 1 Microwave dielectric properties of some low-firing vanadates.

phase	*S.T* (°C)	ε_r	$Q\times f$ (GHz)	τ_f (ppm/°C)	Reference
$BiVO_4$	925	68	8,000	-243	[27]
$Mg_3(VO_4)_2$	950	9.1	64,142	-93.2	[28]
$BiCaVO_5$	820	15.7	55,000	-71	[29]
$BiMgVO_5$	820	18.55	86,860	-65	[29]
$Ca_5Co_4(VO_4)_6$	875	10.1	95,200	-63	[30]
$LiMoVO_6$	640	13.3	12,460	+101.0	[31]
$LiWVO_6$	700	11.5	13,260	163.8	[31]
$NaCa_4V_5O_{17}$	840	9.72	51,000	-84	This work

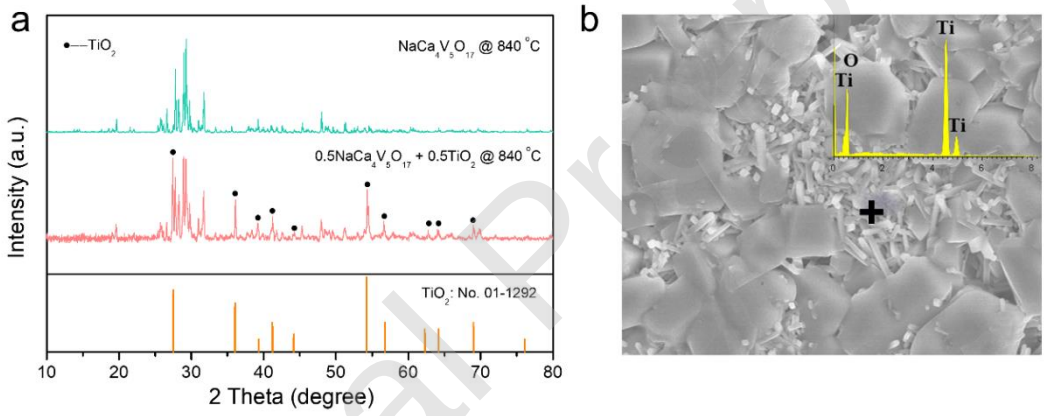

Figure 5 (a) XRD patterns and (b) SEM micrograph of $0.5NaCa_4V_5O_{17}$ + $0.5TiO_2$ composite ceramic sintered at 840 °C (EDS analysis of TiO_2 is shown in the inset of Figure 5b)

Table 2 Sintering temperature (S.T.) and microwave dielectric properties of $(1-x)NaCa_4V_5O_{17}$-$xTiO_2$ composite ceramics

x value	S.T.	ε_r	ε_{rcal}	$Q\times f$ (GHz)	τ_f (ppm/°C)	τ_{fcal}
0	840	9.72	9.72	51,000	-84.3	-84.3
0.1	820	10.5	9.9	45,700	-69.5	-68.9

0.2	820	11.4	10.8	38,800	-57.7	-57.1
0.3	840	12.3	11.7	32,200	-34.6	-34.9
0.4	840	13.1	12.5	25,400	-13.3	-13.7
0.5	840	13.7	13.4	22,500	+3.5	+2.9
0.6	840	14.5	14.1	19,600	+24.3	+23.7

Unfortunately, the large negative τ_f value makes $NaCa_4V_5O_{17}$ ceramics impractical, especially in extreme conditions with large temperature variations. Thus, to achieve temperature stability of resonance frequency against temperature, TiO_2 with a positive τ_f value (~+465 ppm/^{o}C) was chosen as a compensator to form ceramic-ceramic composite [32]. XRD and SEM analysis, given in Figure 5, confirmed no chemical reaction between TiO_2 and $NaCa_4V_5O_{17}$, which was characterized by distinguishing diffraction peaks and grains with distinct sizes. EDS analysis verified the small grains belong to TiO_2. As listed in Table 2, TiO_2 addition significantly changed the dielectric properties of the original $NaCa_4V_5O_{17}$. More specifically, the τ_f value was shifted from negative to positive value and a near-zero value of +3.5 ppm/^{o}C was achieved with 50 mol% TiO_2 addition. A composite ceramic with 50 mol% TiO_2 exhibited balanced dielectric properties with ε_r = 13.7, $Q \times f$ = 22,500 GHz and τ_f = +3.5 ppm/^{o}C.

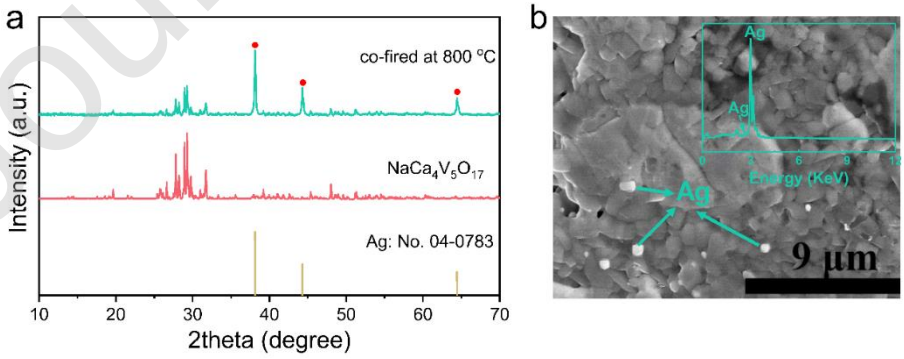

Figure 6 (a) XRD and (b) SEM micrograph of $NaCa_4V_5O_{17}$ cofired with silver

electrode at 840 °C (EDS analysis of Ag is shown in the inset of Figure 6b)

In consideration of the relatively low sintering temperature (840 °C) and excellent microwave dielectric properties, $NaCa_4V_5O_{17}$ can be potentially applicable in low-temperature co-fired ceramics (LTCC) technology, which requires the dielectric materials to be chemically compatible with the electrode materials (silver or aluminum). In order to validate this, $NaCa_4V_5O_{17}$ cofired with the silver electrode at 840 °C for 30 min and characterized with XRD and SEM for a potential reaction between $NaCa_4V_5O_{17}$ and silver. Figure 6 shows the XRD and SEM micrograph of $NaCa_4V_5O_{17}$ cofired with the silver electrode. XRD profiles exhibited the diffraction peaks of $NaCa_4V_5O_{17}$ and silver (as marked by solid circles in Figure 6a) separately confirming no reaction took place between them. On top of that, distinct grains with different sizes and element contrasts were observed in SEM images. EDS revealed the bright smaller grains in the main ceramic matrix to be silver which further confirms a lack of reaction between silver and $NaCa_4V_5O_{17}$. All these results validate the potential application of $NaCa_4V_5O_{17}$ in LTCC technology.

4. Conclusions

$NaCa_4V_5O_{17}$ ceramics were prepared by solid state reaction at relatively low temperatures (780-860 °C). Thermal analysis and X-ray diffraction patterns confirmed the formation of $NaCa_4V_5O_{17}$ at 650 °C. Rietveld refinement verified the phase purity of $NaCa_4V_5O_{17}$ with a triclinic structure *P*-1. SEM images show that dense ceramics with homogenous microstructure were developed. Combined dielectric properties were achieved in the sample sintered at 840 °C with ε_r = 9.72, $Q \times f$ = 51,000 GHz, and

τ_f = -84 ppm/^{o}C. Chemical compatibility with Ag of $NaCa_4V_5O_{17}$ ceramics was also determined based on XRD analysis. Besides, several composite ceramics in the (1-*x*)$NaCa_4V_5O_{17}$-*x*TiO_2 system were synthesized with an attempt to adjust the thermal stability of $NaCa_4V_5O_{17}$. Effectively, a near-zero τ_f ~ +3.5 ppm/^{o}C was accessible in the composite with 50% mol TiO_2 accompanied with ε_r = 13.7 and $Q \times f$ = 22,500 GHz. The intrinsic low sintering temperature, low permittivity along with chemical compatibility with Ag renders the possible application of $NaCa_4V_5O_{17}$ in multilayer electronic devices.

Acknowledgments

Chunchun Li gratefully acknowledges the financial support from Natural Science Foundation of China (No. 51502047), and the Natural Science Foundation of Guangxi Zhuang Autonomous Region (No. 2018GXNSFAA281253).

Reference

[1] M.T. Sebastian, Dielectric Materials for Wireless Communication, 2008.

[2] R.J. Cava, Dielectric materials for applications in microwave communications, J. Mater. Chem. 11 (2001) 54-62.

[3] S. George, M.T. Sebastian, Synthesis and microwave dielectric properties of novel temperature stable high Q, $Li_2ATi_3O_8$ (A = Mg, Zn) Ceramics, J. Am. Ceram. Soc. 30 (2010) 2585-2592.

[4] C.C. Li, C.Z. Yin, J.Q. Chen, H.C. Xiang, Y. Tang, L. Fang, Crystal structure and dielectric properties of germanate melilites $Ba_2MGe_2O_7$ (M = Mg and Zn) with low permittivity, J. Eur. Ceram. Soc. 38 (2018) 5246-5251.

[5] L.X. Pang, D. Zhou, W.G. Liu, Z.M. Qi, Z.X. Yue, Crystal structure and microwave dielectric behaviors of scheelite structured (1-x)$BiVO_4$ -x$La_{2/3}MoO_4$ ($0.0 \leq x \leq 1.0$) ceramics with ultra-low sintering temperature, J. Eur. Ceram. Soc. 38 (2018) 1535-1540.

[6] S.B. Zhang, L.W. Shi, L.Y. Zhang, H.Y. Zhu, W.S. Xia, Synthesis and microwave dielectric properties of new high quality Mg_2NdNbO_6 ceramics, J. Am. Ceram. Soc. 101 (2018) 1014-1019.

[7] R.V. Leite, F.O.S. Costa, M.T. Sebastian, A.J.M. Sales, A.S.B. Sombra, Experimental and numerical investigation of dielectric resonator antenna based on doped $Ba(Zn_{1/3}Ta_{2/3})O_3$ ceramic, Journal of Electromagnetic Waves and Applications, 33 (2019) 84-95.

[8] X.K. Lan, Z.Y. Zou, W.Z. Lu, G.F. Fan, X.H. Wang, X.C. Wang, P. Fu, W. Lei, Novel high Curie temperature $Ba_2ZnSi_2O_7$ ferroelectrics with low-permittivity microwave dielectric properties, Ceram. Int., 42 (2016) 16387-16391.

[9] X.Q. Song, W.Z. Lu, X.C. Wang, X.H. Wang, G.F. Fan, R. Muhammad, W. Lei, Sintering behaviour and microwave dielectric properties of $BaAl_{2-2x}(ZnSi)_xSi_2O_8$ ceramics, J. Eur. Ceram. Soc. 38 (2018) 1529-1534.

[10] C.Z. Yin, H.C. Xiang, C.C. Li, H. Porwal, L. Fang, Low-temperature sintering and thermal stability of Li_2GeO_3-based microwave dielectric ceramics with low permittivity, J. Am. Ceram. Soc. 101 (2018) 4608-4614.

[11] M. T. Sebastian, H. Jantunen, Low loss dielectric materials for LTCC applications: a review,

International Materials Reviews, 53 (2008) 57-90.

[12] J.J. Bian, Y.F. Dong, New high Q microwave dielectric ceramics with rock salt structures:(1-*x*)Li_2TiO_3+*x*MgO system ($0 \leq x \leq 0.5$), J. Eur. Ceram. Soc. 30 (2010) 325-330.

[13] D. Zhou, H. Wang, L.X. Pang, X. Yao, X.G. Wu, Microwave dielectric characterization of a Li_3NbO_4 ceramic and its chemical compatibility with silver, J. Am. Ceram. Soc. 91 (2008) 4115-4117.

[14] M.T. Sebastian, H. Jantunen, Low loss dielectric materials for LTCC applications: a review, Int. Mater. Rev. 53 (2008) 57-90.

[15] B. Liu, L. Yi, L. Li, X.M. Chen, Densification and microwave dielectric properties of $Ca_{1.15}Sm_{0.85}Al_{0.85}Ti_{0.15}O_4$ ceramics with B_2O_3 addition, J. Alloys Compd. 653 (2015) 351-357.

[16] K. Cheng, C.C. Li, H.C. Xiang, Y. Tang, Y.H. Sun, L. Fang, Phase formation and microwave dielectric properties of $BiMVO_5$ (M = Ca, Mg) ceramics potential for low temperature co-fired ceramics application , J. Am. Ceram. Soc. 102 (2019) 362-371.

[17] D.K. Kwon, M.T. Lanagan, T.R. Shrout, Microwave dielectric properties and low-temperature cofiring of $BaTe_4O_9$ with aluminum metal electrode, J. Am. Ceram. Soc. 88 (2005) 3419-3422.

[18] D. Zhou, L.X. Pang, D.W. Wang, I.M. Reaney, Novel water-assisting low firing MoO_3 microwave dielectric ceramics, J. Eur. Ceram. Soc. 39 (2019) 2374-2378.

[19] H.C. Xiang, C.C. Li, Y. Tang, L. Fang, Two novel ultralow temperature firing microwave dielectric ceramics $LiMVO_6$ (M = Mo, W) and their chemical compatibility with metal electrodes, J. Eur. Ceram. Soc. 37 (2017) 3959-3963.

[20] Z.Q. Xie, S.C. Cheng, S.W. Li, H.Q. Ding, $NaCa_4V_5O_{17}$ with isolated V_2O_7 dimer and V_3O_{10} trimer exhibiting a large birefringence, J. Solid State Chem. 269 (2019) 94-99.

[21] S.H. Yoon, D.W. Kim, S.Y. Cho, K.S. Hong, Investigation of the relations between structure and microwave dielectric properties of divalent metal tungstate compounds, J. Eur. Ceram. Soc. 26 (2006) 2051-2054.

[22] R.D. Shannon, Dielectric polarizabilities of ions in oxides and fluorides, J. Appl. Phys., 73 (1993) 348-366.

[23] R.D. Shannon, G.R. Rossman, Dielectric constants of silicate garnets and the oxide additivity

rule, Am. Mineral., 77 (1992) 94-100.

[24] E.S. Kim, B.S. Chun, K.H. Yoon, Dielectric properties of $[Ca_{1-x}(Li_{1/2}Nd_{1/2})_x]1\text{-}yZn_yTiO_3$ ceramics at microwave frequencies, Mater. Sci. Eng: B 99 (2003) 93-97.

[25] X.Q. Song, K. Du, X.Z. Zhang, J. Li, W.Z. Lu, X.C. Wang, W. Lei, Crystal structure, phase composition and microwave dielectric properties of $Ca_3MSi_2O_9$ ceramics, J. Alloys Compd. 750 (2018) 996-1002.

[26] C.C. Li, H.C. Xiang, M.Y. Xu, Y. Tang, L. Fang, Li_2AGeO_4 (A = Zn, Mg): Two novel low-permittivity microwave dielectric ceramics with olivine structure, J. Eur. Ceram. Soc. 38 (2018) 1524-1528.

[27] S.H. Wee, D.W Kim, S.I. Yoo, Microwave Dielectric Properties of Low-Fired ZnNb2O6 Ceramics with $BiVO_4$ Addition, J. Am. Ceram. Soc. 87 (2004) 871-874.

[28] R. Umemura, H. Ogawa, H. Ohsato, A. Kan, A.Yokoi, Microwave dielectric properties of low-temperature sintered $Mg_3(VO_4)_2$ ceramic, J. Eur. Ceram. Soc. 25 (2005) 2865-2870.

[29] K. Cheng, C.C. Li, H.C. Xiang, Y. Tang, Y.H. Sun, L. Fang, Phase formation and microwave dielectric properties of $BiMVO_5$ (M = Ca, Mg) ceramics potential for low temperature co-fired ceramics application, J. Am. Ceram. Soc. 102 (2019) 362-371.

[30] G.G. Yao, P. Liu, X.G.Zhao, J.P. Zhou, H.W. Zhang, Low-temperature sintering and microwave dielectric properties of $Ca_5Co_4(VO_4)_6$ ceramics, J. Eur. Ceram. Soc. 34 (2014) 2983-2987.

[31] H.C. Xiang, C.C. Li, Y. Tang, L. Fang, Two novel ultralow temperature firing microwave dielectric ceramics $LiMVO_6$ (M = Mo, W) and their chemical compatibility with metal electrodes, J. Eur. Ceram. Soc. 37 (2017) 3959-3963.

[32] H.R. Zheng, S.H. Yu, L.X. Li, X.S. Lyu, Z. Sun, S.L. Chen, Crystal structure, mixture behavior, and microwave dielectric properties of novel temperature stable $(1\text{-}x)MgMoO_4\text{-}xTiO_2$ composite ceramics, J. Eur. Ceram. Soc. 37 (2017) 4661-4665.